

SURFACE PLASMON POLARITON MODES IN A CONVEX  
CYLINDER MICRORESONATOR

V. A. TEKKOZYAN<sup>1\*</sup>, A. Zh. BABAJANYAN<sup>1</sup>, Kh. V. NERKARYAN<sup>1\*\*</sup>, K. Lee<sup>2</sup>

<sup>1</sup> *Chair of Microwave Radiophysics and Telecommunications YSU, Armenia*

<sup>2</sup> *Department of Physics and Basic Science Institute for Cell Damage Control, Sogang University, Republic of Korea*

We consider the formation of the surface plasmon polariton whispering gallery modes in the convex cylinder cavity. Developed theoretical model allows obtaining the closed-form expressions for the mode field distributions, resonant frequency, as well as the emitting and dissipative losses in the structure in a broad wavelength range. The obtained results give opportunity to find optimal conditions for efficient emission in convex cylinder cavity and serve as practical guidelines for stimulated emission.

**Keywords:** surface plasmon polariton, convex cylinder, field localization.

**Introduction.** The unique properties of surface plasmon polaritons (SPP) permit further miniaturization of wavelength-scale photonic circuits to sizes that are much smaller than those currently achieved. The features of SPP such as enhanced and spatially confined electromagnetic fields at metal-dielectric interfaces [1, 2] have been exploited in various fields, for example in nanophotonics [3, 4], biosensing [5–9], light generation [10]. Despite the great promise of SPP many applications remained impractical due to high losses resulting from the damping of electromagnetic fields in metals. The active plasmonics, which describes the interaction between active medium and SPP, offers an opportunity to expand SPP-based applications. Furthermore, if the optical gain is high enough to exceed the absorption loss, the compact plasmonic lasers may be realized [11–14]. A step towards quantum nanoplasmonics was proposed by Bergman group, which showed that SPP fields of the nanosystem were quantized and observed their stimulated emission [15, 16]. For the first time a quantum generator for SPP quanta was introduced and the phenomenon of surface plasmon amplification by stimulated emission of radiation (spacer) and its use in nanolens was considered [16]. The examples of recent advances are microscopic lasers based on photonic crystals [17], metal-clad cavities [13] and nanowires [18–20], by means of which the diffraction limit was reached. Because of the strong enhancement of the field induced by excitation of SPP and, consequently, of an increased optical nonlinearity, SPP are particularly suited for providing this functionality.

\* E-mail: [vahant@mail.ru](mailto:vahant@mail.ru)

\*\* E-mail: [knerkar@ysu.am](mailto:knerkar@ysu.am)

With rapidly advancing nanoscale patterning and processing technology, it becomes increasingly practical to generate optical elements from spatially modulated films. Thus, the resonant periodic waveguide is currently receiving considerable research and development interest. Resonant phenomena in structures that include gratings and dielectric waveguides became subjects of investigations both theoretical and experimental.

In the present work an analytical theory of convex cylinder microcavity has

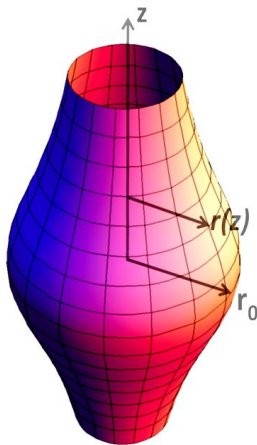


Fig. 1. Schematic view of convex cylinder structure for the SPP.

been developed, with the help of which optimal solutions for the stimulated emission of SPP will be obtained. The problem of significant radiation losses in this cavity with absorption losses of SPP was discussed. The physical constraints imposed by large in-plane extent of the optical field and out-of-plane operation of some of these devices preclude their integration in ultra-compact plasmonic systems.

**Theory.** Under consideration below are the characteristics of SPP, which are localized on the surface of metallic convex cylinder cavity with dielectric permittivity  $\varepsilon_m$ , that is immersed in dielectric medium with permittivity  $\varepsilon_d$ . This structure is schematically represented in Fig. 1.

In the cylindrical coordinate system the wave equation for  $z$ -component of magnetic field is as follows:

$$\frac{\partial^2 H_z}{\partial \rho^2} + \frac{1}{\rho} \cdot \frac{\partial H_z}{\partial \rho} + \frac{1}{\rho^2} \cdot \frac{\partial^2 H_z}{\partial \varphi^2} + \frac{\partial^2 H_z}{\partial z^2} - \varepsilon_{d(m)} \frac{\partial^2 H_z}{c^2 \partial t^2} = 0. \quad (1)$$

We represent the solution in the form

$$H_z = R(\rho)Z(z)e^{i(n\varphi - \omega t)}, \quad (2)$$

which permits to separate the variables in terms of applicability of the adiabatic approximation:

$$\frac{\partial^2 R}{\partial z^2} \ll 1, \quad \frac{\partial R}{\partial z} \ll 1. \quad (3)$$

Changing the variable

$$u = r(z) \ln \left( \frac{\rho}{r(z)} \right). \quad (4)$$

Now consider a metallic convex cylinder with radius  $r(z)$  and a dependence of  $r(z)$  on  $z$  as given by the following expression:

$$r(z) = \frac{r_0}{\sqrt{1 + \alpha^2 z^2}}, \quad (5)$$

where  $r_0 = r(0)$  is the maximum radius of structure and  $\alpha$  is the coefficient, which defines the shape of structure. Using approximation (3), the following wave equation is obtained:

$$Z(z) \frac{\partial^2 R}{\partial u^2} - Z(z) R(\rho, z) \frac{n^2}{r(z)^2} + R(\rho, z) \frac{d^2 Z}{dz^2} e^{\frac{2u}{r_0}} + \varepsilon_{d(m)} \frac{\omega^2}{c^2} Z(z) R(\rho, z) e^{\frac{2u}{r_0}} = 0. \quad (6)$$

When  $|u| \ll r(z)$ , from Eq. (6) we can get:

$$\frac{\partial^2 R}{\partial u^2} - \left[ k^2 - \varepsilon_{d(m)} \frac{\omega^2}{c^2} \right] R = 0, \quad (7)$$

$$\frac{d^2 Z}{dz^2} + \left[ k^2 - \frac{n^2}{r(z)^2} \right] Z = 0. \quad (8)$$

The solution of Eq. (7) is determined by the following expression:

$$R(\rho, z) \approx A e^{-\gamma_{m,d} |\rho - r(z)|}, \quad (9)$$

$$\gamma_m = \sqrt{\frac{n^2}{\rho_0^2} + |\varepsilon_m| \frac{\omega^2}{c^2}} \quad \text{in metal region } (\rho \leq r(z)), \quad (10)$$

$$\gamma_d = \sqrt{k^2 - \varepsilon_d \frac{\omega^2}{c^2}} \quad \text{in dielectric region } (\rho \geq r(z)). \quad (11)$$

From boundary conditions we get the following expression for  $k$ :

$$k = \sqrt{\frac{\varepsilon_d |\varepsilon_m|}{|\varepsilon_m| - \varepsilon_d}} \cdot \frac{\omega}{c}. \quad (12)$$

Finally, from Eq. (5) and (8), we have

$$\frac{d^2 Z}{dz^2} + \left[ \left( k^2 - \frac{n^2}{r_0^2} \right) - \left( \alpha \frac{n}{r_0} \right)^2 z^2 \right] Z = 0. \quad (13)$$

This is the well known quantum mechanical equation for harmonic oscillator. The physical solutions of this equation satisfy the following condition:

$$k_s^2 - \frac{n^2}{r_0^2} = \alpha \frac{n}{r_0} (2s + 1), \quad (14)$$

where  $s = 0, 1, 2, 3, \dots$ . Using Eq. (14), the cavity resonant frequency is determined as

$$\omega_s = \omega_c \sqrt{1 + \beta (2s + 1)}, \quad (15)$$

where  $\omega_c = c \frac{n}{r_0} \sqrt{(|\varepsilon_m| - \varepsilon_d) / (\varepsilon_d |\varepsilon_m|)}$  and  $\beta = \alpha \frac{r_0}{n}$ . Here  $\omega_c$  is the resonant frequency of cylinder cavity (for  $\alpha = 0$ ) with radius  $r_0$ .

**Results and Discussion.** The general solution for Eq. (13) is

$$Z_s = C_s H_s \left( \sqrt{\alpha \frac{n}{r_0}} z \right) e^{-\frac{1}{2} \alpha \frac{n}{r_0} z^2}, \quad (16)$$

where  $H_s$  is the Hermit polynomials and  $C_s$  is a constant.

Using Eqs. (9) and (16), the  $z$ -component for magnetic field in case of fundamental mode ( $s = 0$ ) can be written as:

$$H_{0z} = R_0(\rho, z) Z_0(z) e^{i(n\phi - \omega t)} = A e^{-\gamma_{m,d} |\rho - r(z)|} e^{-\frac{1}{2} \alpha \frac{n}{r_0} z^2} e^{i(n\phi - \omega t)}. \quad (17)$$

Eq. (17) shows that for fundamental mode the propagation length in  $z$ -direction depends on the shape of metal structure and, thus, the speed of decay of  $H_{0z}$  in

$z$ -direction depends on  $\alpha$ ,  $r_0$ ,  $n$  and is localized in  $z_d = \sqrt{2r_0/(\alpha n)}$  region. The faster is the decrease of the structure radius, the shorter is the field propagation range in  $z$ -direction.

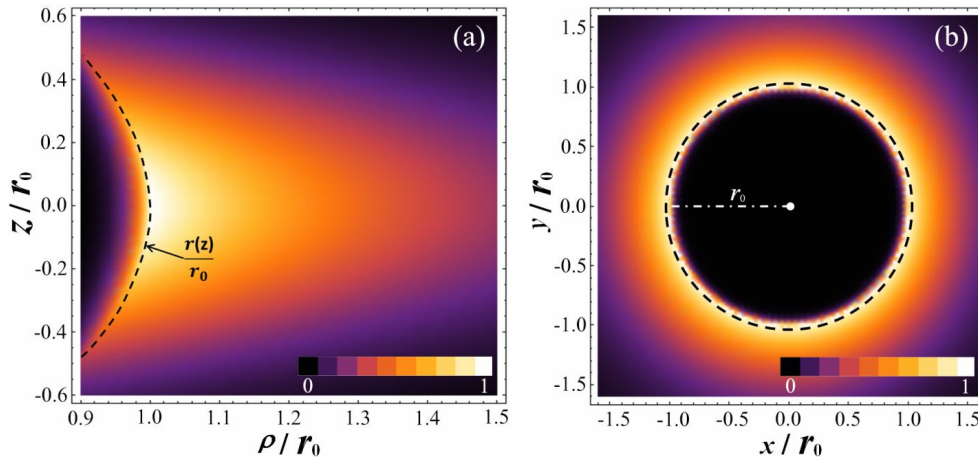


Fig. 2. The stimulated field distribution for  $H_{0z}$  in  $(XZ)$  (a) and  $(XY)$  (b) planes for fundamental mode ( $s = 0$ ) at  $\lambda_{spp} = 1 \mu\text{m}$  for  $\beta = 0.1$  and  $n = 10$ . Dashed line shows the surface of metal structure. The material of structure is gold and the surrounding medium is a dielectric with permittivity  $\epsilon_d = 1$ .

In Fig. 2 the stimulated field distribution for  $H_{0z}$  in (a)  $(XZ)$  and (b)  $(XY)$  planes is shown. The magnetic field is limited (two-scale localized) in a small region near metallic surface at the maximum of  $r$  ( $r = r_0$ ,  $z = 0$ ) and exponentially decrease to the direction of dielectric ( $r > r_0$ ). For example, the magnetic field is localized within  $z_0 = 0.9 r_0$  in  $z$ -direction and  $\rho_0 = 0.4 r_0$  in  $\rho$ -direction for  $\beta = 0.1$  and  $n = 10$ .

In the radiation range  $u \gg r(z)$  we ignored the changes of  $r(z)$  and assumed that  $r(z) \approx r_0$ . With this approximation in the transition zone the following expression is obtained for fundamental mode of magnetic field:

$$H_{0z} \approx B \left( \frac{\epsilon_d}{|\epsilon_m|} \right)^{\frac{1}{2}} \left( 1 - \sqrt{\frac{\epsilon_d}{|\epsilon_m|}} \right)^{n(1+\beta)-\frac{1}{2}} \left( \frac{r_0}{\rho} \right)^{\frac{1}{2}} \exp \{ i[\omega t + n\varphi - q_d \rho + \varphi_0] \}, \quad (18)$$

where  $q_d = \sqrt{\epsilon_d} \omega_0 / c$ .

The other components of the field are obtained from the Maxwell equations.

Then, it is easy to find the radiation part ( $Q_r$ ) of the  $Q$ -factor as

$$Q_r = \frac{1}{4} \left( \frac{|\epsilon_r|}{\epsilon_d} \right)^{\frac{3}{2}} \left( 1 + \frac{1}{\epsilon_d} \right) \left( 1 - \frac{\epsilon_d}{|\epsilon_r|} \right)^{-2n(1+\beta)+1}. \quad (19)$$

Here  $\epsilon_r$  is the real part of dielectric permittivity of metal ( $\epsilon_m = \epsilon_r + i\epsilon_i$ ).

The dissipative part ( $Q_d$ ) of  $Q$ -factor is easily obtained for  $r_0 k_s \gg 1$

$$Q_d = \frac{|\varepsilon_r|^2}{\varepsilon_i \varepsilon_d} \left( 1 - \frac{\varepsilon_d}{|\varepsilon_r|} \right). \quad (20)$$

Finally, for the total quality factor  $Q_t$  we have

$$Q_t = \frac{Q_r Q_d}{Q_r + Q_d}. \quad (21)$$

The optimal conditions for SPP modes in the convex cylinder cavity are determined using Eqs. (19)–(21). In Fig. 3 the dependence of  $Q$ -factors ( $Q_r$ ,  $Q_d$  and  $Q_t$ ) of the convex cylinder cavity on wavelength of SPP is shown.

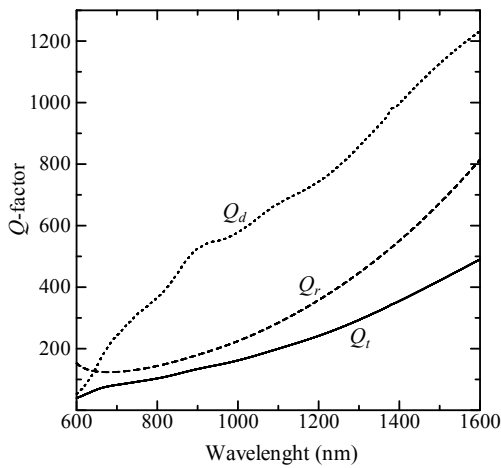


Fig. 3. The dependence of  $Q$ -factors (where  $Q_d$ ,  $Q_r$ ,  $Q_t$  are the dissipative, radiation and total losses respectively) of the convex microcylinder cavity on the wavelength of SPP for  $\beta = 0.1$  and  $n = 10$ . The material of structure is the gold and the surrounding medium is the air.

In the radiation range  $u \gg r(z)$  the fields are similar to those of microcylindrical cavity for SPP with radius  $r_0$  [21]. We have the same situation for  $Q$ -factors as follows from Eqs. (18)–(20) and Fig. 3: the highest value of  $Q$ -factors is achieved when  $|\varepsilon_r| \gg \varepsilon_d, \varepsilon_i$ . Note that the last condition is well satisfied in the infrared region of the spectrum, in particular when  $\lambda_{SPP} \approx \lambda_0 = 1.55 \mu\text{m}$ , which is very important for optical communication systems. The presence of surrounding dielectric medium ( $\varepsilon_d > 1$ ) significantly reduces (about 3 times) the value of  $Q$ -factors, however, the  $Q_t$  is mainly determined by radiation losses. Note also that field localization is better and resonant frequency is higher for higher-order modes than for the fundamental mode. Thus, for efficient stimulated of SPP emission in the convex cavity it is necessary to provide a relatively high value of  $Q$ -factors.

**Conclusion.** The formation of SPP modes in the convex cylinder microcavity is discussed. Analytic solution for wave equation for convex microcylinder metallic structure shows the two-scale localization in  $z$ -direction and in  $\rho$ -direction. The wave field holds in the surface of metal and is not localized in  $z$ -direction due to dependence of the propagation length on  $\alpha$  factor of the structure. Thus, the configuration of convex chamber decides the field distribution and localization.

This structure can serve for elaboration of practical guides to designing SPP microcavity for stimulated emission and strong localization.

*This work was supported by the Parts and Materials International Collaborative R&D Program funded by the MKE of the Republic of Korea.*

Received 18.12.2013

#### REFERENCES

1. **Nerkararyan K.V.** Superfocusing of a Surface Polariton in a Wedge-Like Structure. // *Phys. Lett.*, 1997, A237, p. 103–105.
2. **Gramotnev D.K., Bozhevolnyi S.I.** Plasmonics Beyond the Diffraction Limit. // *Nat. Photon.*, 2010, v. 4, p. 83–91.
3. **Barnes W.L., Dereux A., Ebbesen T.W.** Surface Plasmon Sub-Wavelength Optics. // *Nature*, 2003, v. 424, p. 824–830.
4. **Ozbay E.** Merging Photonics and Electronics at Nanoscale Dimensions Science. // *Plasmonics*, 2006, v. 311, p. 189–193.
5. **Kneipp K., Wang Y., Kneipp H., Perelman L.T., Itzkan I., Dasari R.R., Feld M.S.** Single Molecule Detection Using Surface-Enhanced Raman Scattering. // *Phys. Rev. Lett.*, 1977, v. 78, p. 1667–1670.
6. **Nie S.M., Emory S.R.** Probing Single Molecules and Single Nanoparticles by Surface-Enhanced Raman Scattering. // *Science*, 1997, v. 275, p. 1102–1106.
7. **Lal S., Link S., Halas N.J.** Nano-optics from Sensing to Waveguiding. // *Nat. Photon.*, 2007, v. 1, p. 641–648.
8. **Anker J.N., Hall W.P., Lyandres O., Shah N.C., Zhao J., Van Duyne R.P.** Biosensing with Plasmonic Nanosensors. // *Nat. Mater.*, 2008, v. 7, p. 442–453.
9. **Schultz D.A.** Plasmon Resonant Particles for Biological Detection. // *Curr. Opin. Biotechnol.*, 2003, v. 14, p. 13–22.
10. **Lezec H.J., Degiron A., Devaux E., Linke R.A., Martin-Moreno L., Garcia-Vidal F.J., Ebbesen T.W.** Beaming Light from a Sub-wavelength Aperture. // *Science*, 2002, v. 297, p. 820–822.
11. **Maier S.A.** *Plasmonics: Fundamentals and Applications*. New York: Springer, 2007.
12. **Ambati M., Nam S.H., Ulin-Avila E., Genov D.A., Bartal G., Zhang X.** Observation of Stimulated Emission of Surface Plasmon Polaritons. // *Nano Lett.*, 2008, v. 8, p. 3998–4001.
13. **Hill M.T., Oei Y.S., Smalbrugge B., Zhu Y., DeVries T., Van Veldhoven P.J., Van Otten F.W.M., Eijkemans T.J., Turkiewicz J.P., De Waardt H., Geluk E.J., Kwon S.H., Lee Y.H., Notzel R., Smit M.K.** Lasing in Metallic-Coated Nanocavities. // *Nat. Photon.*, 2007, v. 1, p. 589–594.
14. **Oulton R.F., Sorger V.J., Zentgraf T., Ma R.M., Gladden, Dai L., Bartal G., Zhang X.** Plasmon Lasers at Deep Sub-wavelength Scale. // *Nature*, 2009, v. 461, p. 629–632.
15. **Bergman D.J., Stockman M.I.** Surface Plasmon Amplification by Stimulated Emission of Radiation: Quantum Generation of Coherent Surface Plasmons in Nanosystems. // *Phys. Rev. Lett.*, 2003, v. 90, p. 027402.
16. **Li K., Li X., Stockman M.I., Bergman D.J.** Surface Plasmon Amplification by Stimulated Emission in Nanolenses. // *Phys. Rev.*, 2005, B71, p. 115409.
17. **Altug H., Englund D., Vuckovic J.** Ultrafast Photonic Crystal Nanocavity Laser. // *Nat. Phys.*, 2006, v. 2, p. 484–488.
18. **Johnson J.C., Choi H.-J., Knutsen K.P., Schaller R.D., Yang P., Saykally R.J.** Single Gallium Nitride Nanowire Lasers. // *Nat. Mater.*, 2002, v. 1, p. 106–110.
19. **Duan X., Huang Y., Agarwal R., Lieber C.M.** Single-Nanowire Electrically Driven Lasers. // *Nature*, 2003, v. 421, p. 241–245.
20. **Zimmler M.A., Bao J., Capasso F., Muller S., Ronning C.** Laser Action in Nanowires: Observation of the Transition from Amplified Spontaneous Emission to Laser Oscillation. // *Appl. Phys. Lett.*, 2008, v. 93, p. 051101.
21. **Tekkozyan V., Babajanyan A., Nerkararyan Kh.** Analytic Description of Microcylindrical Cavity for Surface Plasmon Polariton. // *Opt. Commun.*, 2013, v. 305, p. 190–193.